Catal Lett (2009) 128:190–196
DOI 10.1007/s10562-008-9730-z

Photocatalytic Removal of Phenol Under UV Irradiation on WO_x–TiO_2 Prepared by Sol–Gel Method

M. Piszcz · B. Tryba · B. Grzmil · A. W. Morawski

Received: 3 July 2008 / Accepted: 10 October 2008 / Published online: 15 November 2008
© Springer Science+Business Media, LLC 2008

Abstract New WO_x–TiO_2 photocatalysts were prepared via sol–gel method from tetraisopropyl orthotitanate and WO_2. For comparison TiO_2 was also prepared by the same method. These photocatalysts were tested for phenol degradation in an aqueous solution under UV irradiation. Experimentally measured OH radicals formation on WO_x–TiO_2 photocatalysts was quantitatively much higher than on TiO_2, what increased their photocatalytic activity towards phenol decomposition. Band gap of the prepared photocatalysts was calculated from the obtained derivatives of UV–Vis/DR spectra and it was observed that E_g decreased with increasing calcination temperature in both, TiO_2 and WO_x–TiO_2. This was caused by the improving crystallinity of anatase phase and formation of rutile, which had a lower value of E_g than anatase. In general the presence of WO_x in TiO_2 suppressed transformation of anatase to rutile.

Keywords Titanium dioxide · Tungsten oxide · Phenol decomposition · OH radicals

1 Introduction

For many years in photocatalysis titanium dioxide has been attracting the great attention. Application of TiO_2 semiconductor in photocatalytic processes is based on its remarkable activity, chemical stability and also on its non-toxic properties. However, the widespread technological use of this photocatalyst has been hampered by its wide band gap, about 3.2 eV for anatase TiO_2, what causes that only light of wavelengths below 400 nm can excite TiO_2 particles to generate active e^-/h^+ pairs. This wavelight is a small portion of a solar spectrum in ultraviolet (UV) region [1–3]. In order to widen this range and to enhance the photocatalytic efficiency of TiO_2, its modification through deposition of metal particles, selective metal ion doping and surface sensitization, have bee performed [4].

One of doping metal oxide which is widely used is tungsten oxide WO_3. Semiconductor WO_3 may by used as an independent photocatalyst. High rate of phenol degradation on WO_3 was reported by Gondal et al. [5]. They found that small value of the band gap (about 2.8 eV) and decreased pH of the solution improved efficiency of WO_3 in the photocatalytic reaction.

Shifu et al. [6] studied band gaps of WO_3, TiO_2 and coupled WO_3/TiO_2 photocatalysts When WO_3 and TiO_2 form a coupled photocatalyst, the photogenerated electrons of the TiO_2 conduction band can be transferred to the conduction band of WO_3. Since the holes move in the opposite direction from the electrons, photo-generated holes might be trapped within the TiO_2 particle, which makes charge separation more efficient. They concluded that WO_3/TiO_2 coupled photocatalyst exhibited higher photocatalytic activity than TiO_2.

Many researchers tested connected photocatalytic properties of WO_3 and TiO_2 semiconductors. Tungsten oxide doping into TiO_2 caused that the light absorption wavelenght of TiO_2 changed from the near UV to the visible light and improved the yield of photocatalytic reactions by efficient charge separations. Recombination rate of pairs electrons/holes in WO_x–TiO_2 declined due to

The work was presented during the conference 'Catalysis for Society', Krakow, May 11–15, 2008.

M. Piszcz (✉) · B. Tryba · B. Grzmil · A. W. Morawski
Institute of Chemical and Environment Engineering, Szczecin University of Technology, ul.Pułaskiego 10, 70-322 Szczecin, Poland
e-mail: mpiszcz@ps.pl

the existence of WO_3 doped in TiO_2 [3, 7, 8]. Many characteristics WO_x–TiO_2 photocatalysts showed that tungsten oxide hindered the growth of TiO_2 particles and greatly increased the transformation temperature from anatase to rutile during sintering. WO_x can form non-stoichiometric tungsten oxide W_xO_y with W^{n+} ($4 < n < 6$) which easily substitutes Ti^{4+} in the lattice of TiO_2, because ions W^{n+} and Ti^{4+} have similar radius [3, 6–14].

Li et al. [7] reported that coupled WO_3/TiO_2 photocatalysts prepared by a sol–gel method can form stoichiometric solid solution of $W_xTi_{1-x}O_2$. Solid solution of $W_xTi_{1-x}O_2$ can produce a tungsten impurity energy level and depend from the amount of WO_3. When the content of WO_3 is lower than its optimum ratio, tungsten impurity energy level would be a separation center. On the contrary, when the content of WO_3 is higher than its optimum ratio, tungsten impurity energy level would be a combination center. So, the activity of the photocatalyst increases with the increase of the amount of doped-WO_3; but it will decrease remarkably when the doped-WO_3 is higher than a certain amount [15].

Li et al. [7] and Song et al. [3] have prepared WO_x doped TiO_2 photocatalysts by two methods, sol–gel and sol-mixing with different concentration of WO_x in TiO_2. They used these photocatalysts for photodegradation of a dye methylene blue in an aqueous solution. They found that by doping WO_3 the degradation rate was enhanced under visible light irradiation. The yield of photocatalytic reaction was improved by efficient charge separation. Li et al. and Song et al. [3, 7] concluded that the optimum dosage of WO_x in TiO_2 was 3% and 1%, respectively.

Other authors prepared WO_x–TiO_2 by above-mentioned methods too, but they mixed TiO_2–WO_3 oxides with different molar ratios. New photocatalysts were calcined at different temperatures and in different time in air. They also found higher photocatalytic activity of coupled WO_x–TiO_2 photocatalysts. Compared with TiO_2, the photo-excited wavelength range of coupled photocatalyst showed a red shift and increased intensity of the light absorption [6, 16, 17].

In the present study WO_x–TiO_2 samples were prepared by a sol–gel process and their photocatalytic activity was studied by photodegradation of phenol in the aqueous solution under UV irradiation.

2 Experimental

2.1 Photocatalyst Preparation

WO_x–TiO_2 photocatalysts were prepared by a sol–gel method. Tetraisopropyl orthotitanate ($C_{12}H_{28}O_4$)Ti (Merck) and WO_2 (Aldrich) were used as a starting materials. The calculated amount of WO_x in TiO_2 was 3 wt%. Firstly 10 mL $C_{12}H_{28}O_4Ti$ was mixed with the same amount of isopropanol (POCH Gliwice), and 0.084 g WO_2 was dissolved in 100 mL H_2O_2 (Scharlau). Then WO_2/H_2O_2 solution was added drop by drop to the $C_{12}H_{28}O_4Ti$ sol under vigorous stirring on the magnetic stirrer, and WO_x–TiO_2 gel was formed. The resulting colloidal mixture was subjected to hydrolysis process at 70 °C for 1 h and then at 100 °C until the water being evaporated completely [3, 7, 8]. This process was performed in water bath. The obtained WO_x–TiO_2 yellowish powder was dried in an oven and was calcined from 400 to 800 °C for 1 h. For comparison, TiO_2 samples without WO_x and WO_x without TiO_2 were prepared according to the above procedure. All chemicals used in this work were of analytical grade.

2.2 Characterization of TiO_2 and WO_x–TiO_2 Photocatalysts

Analysis of OH radicals formation on the sample surface under UV irradiation was performed by a fluorescence technique using coumarin. This reagent readily reacts with OH radicals to produce highly fluorescent product, 7-hydroxycoumarin, according to the reaction below:

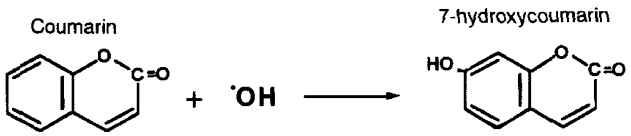

The intensity of the peak attributed to 7-hydroxycoumarin is known to be proportional to the amount of OH radicals formed. The product of coumarin hydroxylation, 7-hydroxycoumarin was determined by means of spectrofluorymeter Hitachi F-2500, the fluorescence spectra were recorded at excitation wavelength 332 nm for emission spectra in the range of 330–600 nm with λ_{max} at around 460 nm [18–20].

The phases composition in the WO_x–TiO_2, TiO_2 and WO_x samples were analysed by XRD powder diffraction. Measurements were performed in X'Pert PRO diffractometer of Philips Company, with CuKα lamp (35 kW, 30 mA). Obtained XRD patterns were compared with Join Committee on Powder Diffraction Standards (JCPDS) cards.

The band gap energies of samples were determined using UV–Vis/DR spectrometer (Jasco, Japan). Diffuse reflectance spectra were recorded in the range of 230–800 nm with $BaSO_4$ as a reference. First derivative ($dR/d\lambda$) was determined from the obtained spectrum, the wavelength with a maximum absorbance (λ_{max}) was used for E_g calculation. E_g was calculated according to the equation:

$$E_g = h \times (c/\lambda_{max})$$

where E_g is the band gap energy (eV); h is the Planck's constant; c is the light velocity (m/s) and λ_{max} is the wavelength determined at max absorbance (nm).

Particle size of photocatalysts was measured in Zetasizer Nano-ZS of Malvern Company. Calgon was used as a dispergant. Calgon is a non ionic surfactant, which makes a homogeneous and well dispersed solution of an analysed suspended catalyst.

The SEM measurements with EDS analysis were performed in JOEL electron scanning microscope, in order to check the microstructure of the photocatalyst surface.

2.3 Photocatalytic Activity Test

The photoactivities of prepared WO_x–TiO_2 samples were tested for phenol decomposition under UV irradiation. Each time, for the photocatalytic test, the breaker with 500 mL of a phenol solution of concentration around 0.02 g/L and 0.1 g of photocatalyst were used. The solutions were first magnetically stirred in a dark for 3 h until the adsorption of phenol into the photocatalyst particles was estimated and then were irradiated for 9 h under UV from the top of the breaker. Scheme of a reactor used is presented in Fig. 1. To determine the change of phenol concentration in the solution after adsorption and during UV irradiation, a few milliliters of the solution was taken from the reaction mixture, centrifuging, and loaded in UV–Vis spectrophotometer (Jasco V-530, Japan). The phenol concentration was measured from the absorbance at the wavelength of 270 nm by using a calibration curve. As a source of UV six lamps of Philips company with power of 20 W each were applied. These lamps emit the radiation at the visible region of about 100 W/m^2 and at UV range of 154 W/m^2 intensities, in the range of 312–553 nm with a maximum at around 350 nm [21, 22].

Plot of relative concentration of phenol in the solution against irradiation time was approximated to be linear, the slope of the linear relation, i.e., rate constant k_{phenol}, was determined on each sample and used as a measure of the photocatalytic activity of the sample. In the same way the rate of OH radicals formation k_{OH} was determined for each sample.

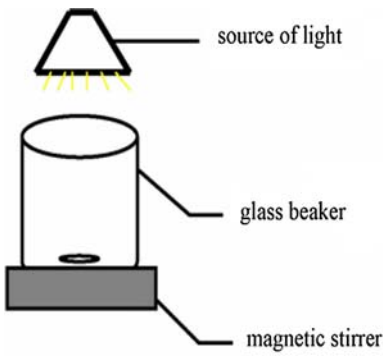

Fig. 1 Scheme of a photocatalytic reactor used for phenol decomposition

3 Results

3.1 XRD Measurements

XRD patterns of TiO_2 and WO_x doped TiO_2 samples are shown in Fig. 2a and b, respectively. After heating at 400 °C single phase was anatase. With increasing the heat-treament temperature to 800 °C anatase was partly transformed to rutile, as shown in diffractogramms in Fig. 2a. For all WO_x–TiO_2 samples, no other phases were detected, except anatase in low temperature, and rutile at high temperatures, as shown in Fig. 2b. WO_3 phase was not detected in the diffraction patterns. In Fig. 2c diffractogramms of crystallized WO_3 samples obtained after dissolving WO_2 in H_2O_2 and calcination at 400 and 600 °C, are presented. After calcination reflexes from WO_3 were observed. Two kinds of WO_3 crystals were identified: monoclinic and anorthic, according to the JCPDS files, No. 87-2382, 72-1465 for monoclinic and 76-1734 for anorthic. In sample calcined at 400 °C dominant phase was anorthic WO_3 and small quantity monoclinic WO_3, but at 600 °C whole anorthic WO_3 was transformed to monoclinic WO_3.

Reflexes came from WO_3 and anatase are situated close together, in the 2θ range about 25° and 53–56°. It could cause that WO_3 phase was screened, and not found in diffractograms of WO_x–TiO_2 samples.

3.2 Band Gap Energy

The band gap of the prepared photocatalysts are presented in Table 1. With increasing the calcination temperature, value E_g slowly decreases from about 3.3 to 3 eV in both, TiO_2 and WO_x–TiO_2 photocatalysts. It was caused by the presence of higher quantity of rutile which was formed at higher temperatures of heat-treatment. Rutile has lower value E_g than anatase.

3.3 Particle Size

In Table 1 particle size of TiO_2 and WO_x–TiO_2 photocatalysts are listed. Doping of WO_x to TiO_2 caused increase their particle size. Heating TiO_2 to 500 °C caused growing of the particles, what was caused by the growing of anatase and a little rutile crystals, above this temperature up to 800 °C the particle size was diminished, probably because of the lower tendency to form agglomerates. The same

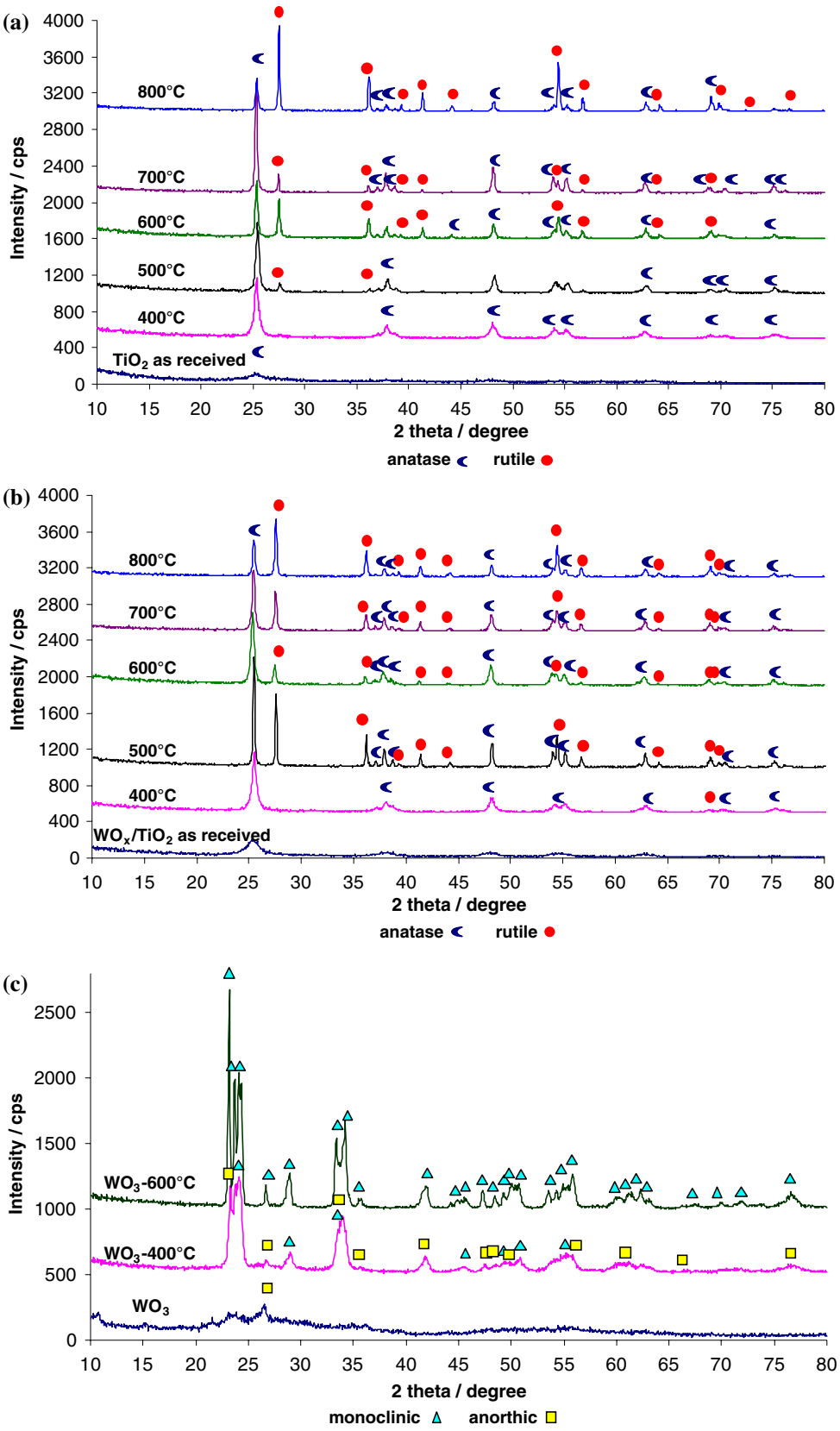

Fig. 2 XRD patterns of prepared **a** TiO_2, **b** WO_x–TiO_2 and **c** WO_3 photocatalysts, as received and calcined at different temperatures

Table 1 Characteristics of TiO_2 and WO_x–TiO_2 photocatalysts

Catalyst	E_g (eV)	Particle size (nm)	k_{OH} (min^{-1})	k_{phenol} (h^{-1})
TiO_2				
as received	3.37	147	0.4	0
400 °C	3.08	200	26.9	5
500 °C	3.04	262	29	7.3
600 °C	2.98	164	16.4	1.7
700 °C	3.04	150	18	0.2
800 °C	3	150	23	0
WO_x–TiO_2				
as received	3.29	296	12.2	2.1
400 °C	3.27	299	51.3	5.3
500 °C	3.28	329	73	4.4
600 °C	3.08	288	147.7	7.7
700 °C	3.07	154	125.6	11.2
800 °C	3.05	133	40.5	4.3

dependence can by observed in case WO_x–TiO_2 photocatalysts. With increasing heat-treatment temperature to 500 °C, the particle size was increased to 329 nm, however at 800 °C the average particle size decreased to 133 nm.

For comparison, particle size of WO_x as recived and calcined at 400 and 600 °C was also measured. With increasing calcination temperature particle size decreased, having the average size of 262, 213 and 150 nm for WO_x, WO_x-400 and WO_x-600, respectively.

The morphology of the photocatalyst surface was observed on the SEM micrographs. Scanning electron micrographs of WO_x calcined at 600 °C and WO_x–TiO_2 calcined at 700 °C photocatalysts are presented in Fig. 3a, b. As can be seen in both cases catalysts grains stick together and create agglomerates. In case of WO_x, the particles are larger and exist in loose aggregates. Distribution of particle size varies much, from around 100 to 500 nm. In case of WO_x–TiO_2 the size of particles gets smaller (in the range of 80–400 nm with domination of particles around 200 nm). TiO_2 particles are smaller then WO_x, therefore average size particle is lower for WO_x–TiO_2 then TiO_2. In case WO_x–TiO_2 the particle size distribution is more uniform. It was measured by EDS that the ratio of W:Ti is 1% atomic and 3.9% by weight.

3.4 OH Radicals Measurements

In Fig. 4 the formation of OH radicals on the photocatalysts surface during UV irradiation is presented. The increase of OH radicals formation with time of UV irradiation can be observed. Quantitatively higher amounts of OH radicals were formed on WO_x–TiO_2 than TiO_2 photocatalysts, as shown in Fig. 4a, b. High rates of OH radicals formation were observed on the surface of TiO_2 and WO_x–TiO_2 photocatalysts calcined at 500 and 600 °C, respectively, whereas the low rates of OH radicals formation were observed in case of both, TiO_2 and WO_x–TiO_2 obtained before calcination. The rate constants of OH radicals formation (k_{OH}) are presented in Table 1. The presence of WO_x in TiO_2 increased the rate of OH radicals formation, however it was decreasing with appearing of rutile phase.

Higher rates of OH radicals formation on WO_x–TiO_2 than TiO_2 samples be caused by retarding recombination rate in TiO_2 semiconductor by WO_3.

3.5 Decomposition of Phenol Under UV Irradiation

Adsorption and decomposition of phenol on TiO_2 and WO_x–TiO_2 samples under UV irradiation are shown in Fig. 5. As shown in Fig. 5a, b, no phenol adsorption on the surface of the photocatalysts was observed within 3 h in case of both, TiO_2 and WO_x–TiO_2 samples. TiO_2 sample obtained before and after calcination at 800 °C showed no high photoactivity for phenol decomposition. High rates of phenol degradation were observed on TiO_2 and WO_x–TiO_2 calcined at 500 and 700 °C, respectively. In case of both, TiO_2 and WO_x–TiO_2 photocatalyst, samples which have large amount of rutile phase showed decrease their photocatalytic activity.

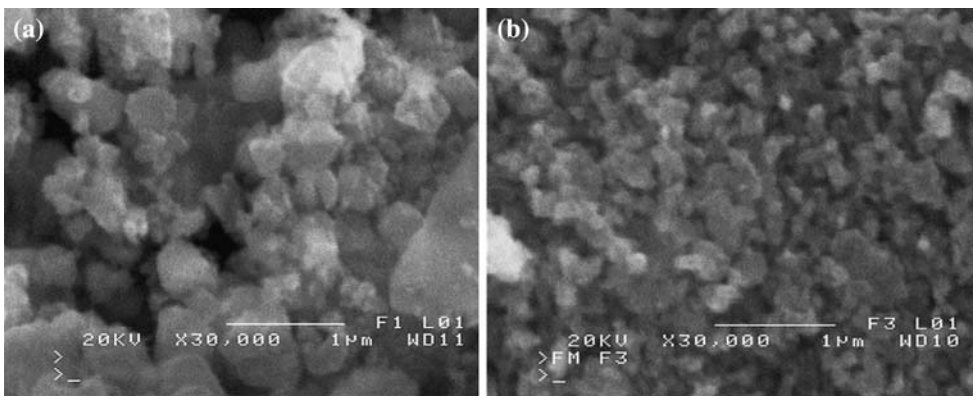

Fig. 3 Scanning electron micrographs of sample. **a** WO_3-600 °C, **b** WO_x–TiO_2-700 °C

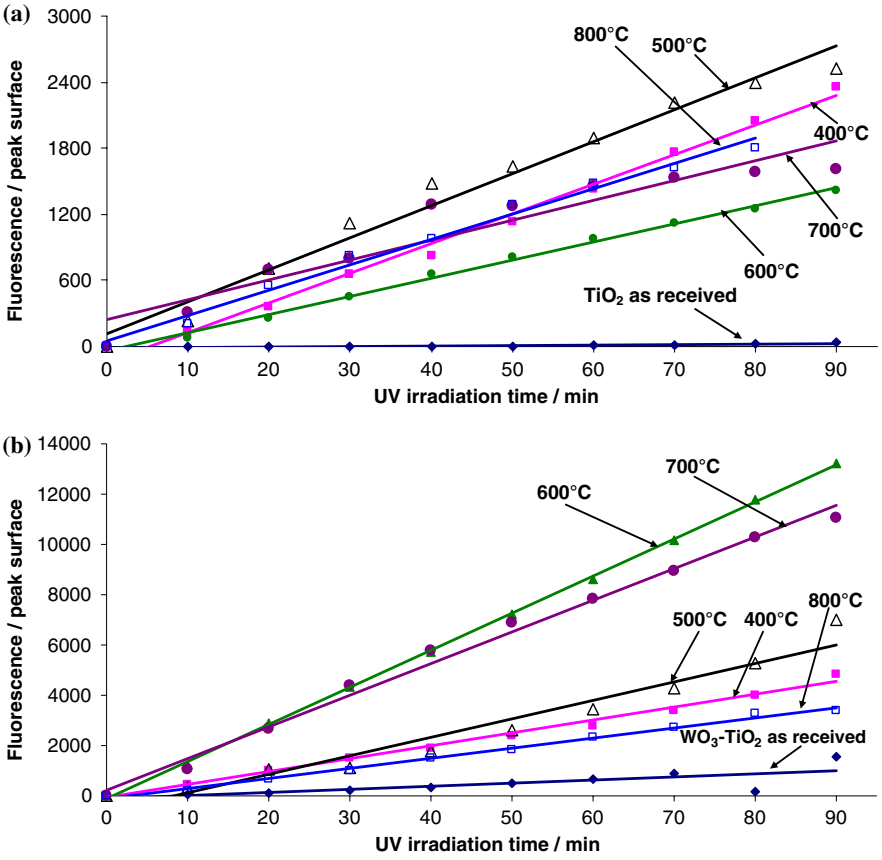

Fig. 4 Formation of OH radicals under UV radiation on the photocatalyst surface. **a** TiO_2, **b** WO_x–TiO_2

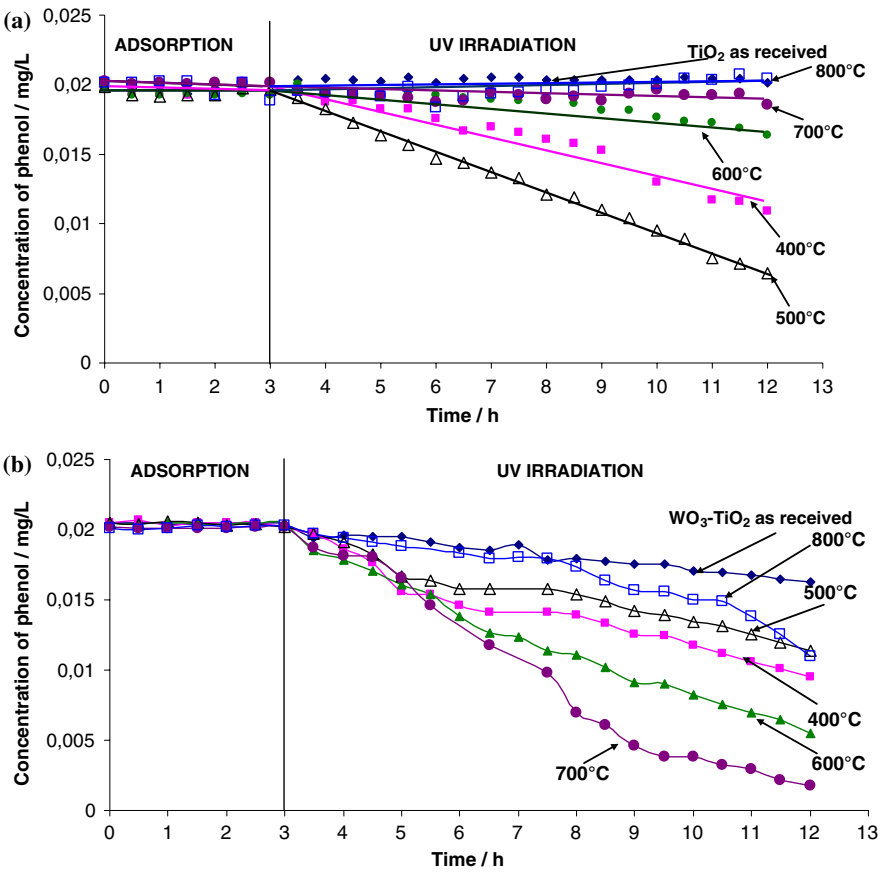

Fig. 5 Phenol decomposition under UV irradiation on photocatalysts. **a** TiO_2, **b** WO_x–TiO_2

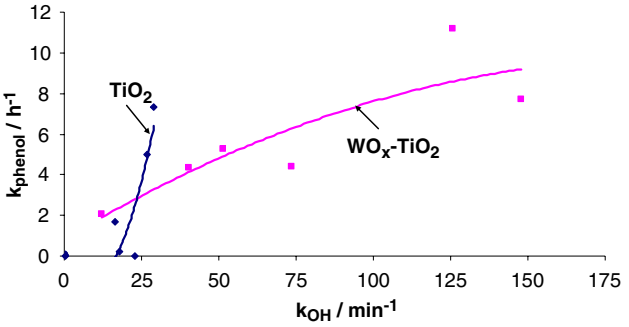

Fig. 6 Dependence of the rate constant of phenol decomposition from the rate constant of OH radicals formation

The relation between rate of OH radicals formation and rate of phenol decomposition is shown in Fig. 6. In general, with increasing rate of OH radicals formation on the TiO_2 and WO_x–TiO_2 photocatalysts surface, the rate of phenol decomposition increases, however in case of TiO_2 samples small increase in a k_{OH} results in a high increase of k_{phenol}. It can be suggested that although the recombination rate in WO_x–TiO_2 photocatalysts was slowed down and yielding of OH radicals formation was increased, this is not only factor influences the phenol decomposition.

4 Conclusions

Doping WO_3 to TiO_2 increased the rate of OH radicals formation on the photocatalyst surface. Transformation of anatase to rutile caused decreasing the energy of the band gap. Proceeding higher transformation of anatase to rutile resulted in decreasing of both, OH radicals formation and rate of phenol decomposition. It could be caused by enhancing the recombination rate between photogenerated carriers. Phenol decomposition goes quickly on the photocatalysts which show high efficiency in OH radicals formation, however this is not only factor influences the rate of phenol decomposition.

Doping WO_3 to TiO_2 caused retarding the recombination between excited electrons–holes pairs what resulted in higher efficiency of OH radicals formation, and consequently higher activity for phenol decomposition.

Acknowledgments This work was supported by the research project from the Ministry of Science and Higher Education Nr COST/299/2006 for 2007–2010.

References

1. Poulios I, Tsachpinis I (1999) J Chem Technol Biotechnol 74:349
2. Araña J, Doña-Rodríguez JM, Tello Rendón E, Garriga C, Cabo I, González-Díaz O, Herrera-Melián JA, Pérez-Peña J, Colón G, Navío JA (2003) Appl Catal B 44:161
3. Song H, Jiang H, Liu X, Meng G (2006) J Photochem Photobiol A 181:421
4. Shen M, Wu Z, Huang H, Du Y, Zou Z, Yang P (2006) Mater Lett 60:693
5. Gondal AM, Sayeed MN, Alarfaj A (2007) Chem Phys Lett 445:325
6. Shifu C, Lei C, Shen G, Gengyu C (2005) Powder Technol 160:198
7. Li XZ, Li FB, Yang CL, Ge WK (2001) J Photochem Photobiol A 5744:1
8. Yang H, Shi R, Zhang K, Hu Y, Tang A, Li X (2005) J Alloy Comp 398:200
9. Xiu Q, Yuan Xiao H, Sheng Li W, Sheng Li W, Qing Na Y, Ping Zhou X (2005) Appl Catal A 290:25
10. Keller N, Barraud E, Bosc F, Edwards D, Keller V (2007) Appl Catal B 70:423
11. Bosc F, Edwards D, Keller N, Keller V, Ayral A (2006) Thin Solid Films 495:272
12. Radecka M, Sobas P, Wierzbicka M, Rekas M (2005) Physica B 364:85
13. Alemany LJ, Larrubia MA, Jimènez MC (1997) React Kinet Catal Lett 60:41
14. Guo Y, Quan X, Lu N, Zhano H, Chen S (2007) Environ Sci Technol 41:4422
15. Ke D, Liu H, Peng T, Liu X, Dei K (2008) Mater Lett 62:447
16. Komornicki S, Radecka M, Sobaś P (2004) Mater Res Bull 39:2007
17. Yang H, Zhang D, Wang L (2002) Mater Lett 57:674
18. Ishibashi K, Fujishima A, Watanabe T, Hashimoto K (2000) Electrochem Commun 2:207
19. Dai Q, Wang D, Yuan Ch (1998) Supramol Sci 5:469
20. Tryba B, Toyoda M, Morawski AW, Nonaka R, Inagaki M (2007) Appl Catal B 71:163
21. Janus M, Morawski AW (2007) Appl Catal B 75:118
22. Tryba B, Morawski AW, Inagaki M (2003) Appl Catal B 46:203